

food for benthic communities, resulting in high benthic biomass (Grebmeier et al., 1988, 2006, 2015; Grebmeier, 2012). Consequently, large benthic feeders at high trophic levels, such as grey whales and walrus, also congregate there (Feder et al., 2005). Such a region of high biological activity is called a biological hotspot.

5 The Arctic has rapidly lost its summer sea ice cover over recent decades (Stroeve et al., 2007; Comiso et al., 2008; Kwok et al., 2009), which may significantly change ocean conditions and marine biological activities. However, the effects of extreme ice retreats and delayed sea ice formation in late autumn on primary production are uncertain in the Pacific Arctic including the Chukchi Sea, whereas clear changes have
10 occurred in the ranges of zooplankton, benthic organisms, and fish species in summer, as well as through loss of sea ice as habitat and platforms for marine mammals (Grebmeier et al., 2010, 2015; Grebmeier, 2012). Primary productivity in the Arctic has increased in recent years, as estimated using satellite data, due to an accelerated extension of the open water area and a longer ice-free season (e.g. Arrigo et al., 2008; Pabi et al., 2008). In contrast, seasonal field measurements in the Chukchi Sea during
15 the ice-free season in summer/fall indicate a substantial decrease in recent primary productivity compared to estimates in the 1980s (Lee et al., 2007, 2013). One of the reasons for the recent low primary productivity obtained from in situ measurements may be the large annual variation related to spatial and temporal changes in biogeochemical processes (Lee et al., 2007). Therefore, long-term monitoring using moorings with chemical and biological sensors is necessary along with ship-based hydrographic and biogeochemical surveys to better understand the responses of marine ecosystem to ongoing environmental changes in the Chukchi Sea. The southern Chukchi Sea is
20 a suitable location for such long-term monitoring because the site is one of the most biologically productive regions and thus is in a state of significant transition, with not only environmental but also potentially economic and social consequences.

The recent loss of Arctic sea ice may also induce a second bloom in fall (fall bloom) because the delayed freeze-up and increased exposure of the sea surface to wind stress causes significant wind-driven vertical mixing and upward supply of nutrients,

16361

resulting in increased phytoplankton biomass. Ardyna et al. (2014) used satellite data to show that the frequency and area of fall blooms have increased recently throughout the Arctic. Nishino et al. (2015) reported fall bloom during strong wind events in the northern Chukchi Sea based on observational evidence. The increase in biomass
5 during fall bloom could accompany changes in phyto- and zooplankton communities and may impact higher trophic levels in the ecosystem (Yokoi et al., 2015; Matsuno et al., 2015). However, the fate of the fall bloom (e.g. when it begins, the trigger, how long it continues, and the mechanism maintaining it) is unclear. Seasonal monitoring of phytoplankton biomass using water mass characteristics may provide answers to such
10 questions.

Here, we analysed mooring and ship-based data obtained from a biological hotspot in the southern Chukchi Sea to understand the water mass characteristics (and temporal changes thereof) that influence phytoplankton biomass and productivity. Mooring data, including temperature (T), salinity (S), dissolved oxygen (DO), chlorophyll a (Chl a), and turbidity near the bottom of the biological hotspot in the southern Chukchi
15 Sea were collected from July 2012 to July 2014 for the first time. The data were used to examine changes in water mass characteristics and phytoplankton biomass associated with spring and fall blooms in this biological hotspot. Hydrographic and biogeochemical surveys (conductivity-temperature-depth [CTD] and water sampling) were conducted
20 across the biological hotspot during late summer to fall 2012 and 2013. We focused on the biogeochemical parameters DO, Chl a , turbidity, and nutrients to study the biogeochemical processes that maintain the biological hotspot until late summer and fall, and their differences between the 2 years. The effect of sea ice meltwater on primary productivity is also discussed in association with stratification of the water column.

16362

2 Data and methods

2.1 Mooring data

We deployed and recovered three temporally sequenced moorings (named SCH-12, SCH-12-2, and SCH-13; Table 1) from 16 July 2012 to 19 July 2014 to acquire T , S , DO, Chl a , and turbidity time-series near the bottom of a biological hotspot located in Hope Valley of the southern Chukchi Sea (Fig. 1). A MicroCAT C-T Recorder, SBE 37-SM (Sea-Bird Electronics, Bellevue, WA, USA) was used to acquire the T and S data. Maximum drift in the sensors over 1 year were $0.002\text{ }^{\circ}\text{C}$ for temperature and 0.01 for salinity in pre- and post-calibration comparisons. The AROW-USB phosphorescent DO sensor was used (JFE Advantech Co., Ltd., Kobe, Japan). The sensor was calibrated using oxygen-saturated and anoxic water to determine the linear relationship between them with $\pm 2\%$ accuracy. Fluorescence and backscatter were measured to obtain the Chl a and turbidity data, respectively, using ACLW-USB sensors (JFE Advantech). Chl a nonlinearity between 0 and 200 mg m^{-3} was $\pm 1\%$. The turbidity sensor was calibrated by the manufacturer using formazin standard solutions, and the results were expressed in formazin turbidity units (FTUs). Accuracy of the turbidity sensor was ± 0.3 FTU or $\pm 2\%$. The data were recorded every hour and were smoothed using a running 24 h mean after removing spike noise. Because the DO value obtained on 1 September 2013 from the third mooring (SCH-13) was much higher than that from the water sample collected at the nearest location and time to the mooring data acquisition, we subtracted the excess value of $69\text{ }\mu\text{mol kg}^{-1}$ from the SCH-13 mooring DO data collected from 20 July 2013 to 19 July 2014.

To analyse the mooring data, we used the definitions of water masses from previous studies. The bottom waters in the Chukchi Sea that originate from the Pacific Ocean in summer and winter are characterised by T and S . In summer, they can be classified into three water masses: Anadyr Water ($S > 32.5$, $T = -1.0$ – $1.5\text{ }^{\circ}\text{C}$) in the west, Bering Shelf Water ($S = 31.8$ – 32.5 , $T = 0$ – $4\text{ }^{\circ}\text{C}$) in the centre, and Alaskan Coastal Water (ACW; $S < 31.8$, $T > 4\text{ }^{\circ}\text{C}$) near the Alaskan coast (Coachman et al., 1975; Coach-

16363

man, 1987; Grebmeier et al., 1988). As the Anadyr and Bering Shelf Waters are usually not distinct in the Chukchi Sea, the combined water mass is called the Bering Shelf-Anadyr Water (BSAW). In winter, the water mass called Bering Winter Water (BWW; $S = 32.4$ – 34.0 with near freezing temperature) occupies the Chukchi Sea (Coachman and Barnes, 1961; Kinney et al., 1970).

2.2 Ship-based data

Ship-based hydrographic and biogeochemical surveys were conducted in the Chukchi Sea and Canada Basin from 13 September to 4 October 2012 and from 31 August to 4 October 2013 on board the R/V *Mirai* of the Japan Agency for Marine-Earth Science and Technology, JAMSTEC (Fig. 1). Detailed descriptions of the 2012 and 2013 R/V *Mirai* cruises, including the above-mentioned moorings, are provided in the cruise reports (Kikuchi 2012 and Nishino 2013, respectively), and the data will be open to the public via the JAMSTEC website (<http://www.godac.jamstec.go.jp/cruisedata/mirai/e/index.html>). We also used data obtained from cruises of the R/V *Mirai* in 2004, 2008, and 2010 to compare to the data from 2012 and 2013, which were downloaded from the JAMSTEC website. The R/V *Mirai* survey periods for the area north of the Bering Strait in each year are listed in Table 2.

A CTD (SBE9plus; Sea-Bird Electronics) and a carousel water-sampling system with 36 Niskin bottles (12 L) were used to collect data. In addition, DO, light transmission, fluorescence, and photosynthetically active radiation sensors were attached to the CTD system. Seawater samples were collected to measure S , DO, total alkalinity, nutrients (nitrate, nitrite, phosphate, silicate, and ammonium), Chl a , primary productivity, and other chemical and biological parameters.

Bottle S samples were analysed following the Global Ocean Ship-based Hydrographic Investigations Program (GO-SHIP) Repeat Hydrography Manual using a Guideline AUTOSAL salinometer and International Association for the Physical Sciences of the Oceans standard seawater as reference material (Kawano, 2010). Precision values of the salinity measurements in 2012 and 2013 were 0.0060 and 0.0068 ,

16364

3 Results

3.1 Mooring data

3.1.1 *T* and *S*

As described in Sect. 2.1, the bottom waters in the Chukchi Sea are classified into ACW, BSAW, and BWW. The *T* and *S* characteristics from the mooring data (Fig. 2a) indicate a seasonal change in water masses similar to BSAW and BWW. The BSAW occupied the bottom of the mooring site until November 2012, but it was warmer and fresher during July–October 2013 compared with 2012. The BWW was present during winter from January to May 2013 and from February to April 2014.

3.1.2 DO and turbidity

DO concentration (blue line in Fig. 2b) seemed to vary in response to the change in water masses. The BWW has high DO concentrations ($> 300 \mu\text{mol kg}^{-1}$) because the water undergoes cooling and convection in winter with oxygen supplied from the atmosphere. In contrast, there is a wide range of DO concentrations in BSAW. DO concentration was high ($\sim 300 \mu\text{mol kg}^{-1}$) in the beginning when the BSAW occupied the mooring site in July. Then it decreased sharply over time and had minimum values ($\sim 100 \mu\text{mol kg}^{-1}$) between September and November 2012 and between August and October 2013. During these times of each year, turbidity was maximum (10–15 FTU) in an annual cycle (red line in Fig. 2b). The decrease in DO concentration and the increase in turbidity were probably related to biogeochemical processes, i.e. the deposition of particles at the bottom and decomposition of organic matter transported with the particles. This point will be discussed in Sect. 4.1.

16367

3.1.3 Chl *a*

The Chl *a* mooring data captured phytoplankton blooms, as indicated by high Chl *a* concentrations in spring to early summer and autumn (Fig. 2c). Chl *a* concentration increased sharply in May, when sea ice still remained in the area, and the high concentration continued until July, suggesting a spring bloom including a bloom of ice algae. The DO concentration (blue line in Fig. 2b) at the onset of the spring bloom in May increased with the increase in Chl *a*. These DO and Chl *a* increases are consistent with the oxygen production accompanying phytoplankton photosynthetic activity. Relatively high Chl *a* concentrations ($> 1 \text{ mg m}^{-3}$) were found in September–October 2012 and August–October 2013, although the concentration was much lower than that during the spring bloom. The high concentrations during these periods probably reflected fall blooms. A time series of the turbidity (red line in Fig. 2b) data showed two peaks in accordance with annual variation in Chl *a* concentration, i.e. high turbidity in spring to early summer and autumn. However, turbidity was higher in autumn than in spring to early summer, despite lower Chl *a* concentrations in autumn. The high turbidity in autumn suggests that the turbid water contained not only phytoplankton but also other biogenic and lithogenic particles.

3.2 Ship-based data

3.2.1 Chl *a* and primary productivity

The hydrographic and biogeochemical surveys were conducted in the Chukchi Sea and the Canada Basin during September to early October 2012 and 2013, when the fall blooms were characterised by high Chl *a* and turbidity with low DO concentrations. The spatial distribution of Chl *a* integrated over the water column in 2012 (Fig. 3a) showed that the quantity of Chl *a* was relatively high in the Bering Strait, Hope Valley, and Barrow Canyon, where primary productivity in the water column was also high compared to that in the central Chukchi Sea and the Canada Basin in 2012 (Fig. 3b).

16368

The quantity of Chl *a* in the water column in 2013 was higher everywhere compared to 2012, and the highest quantity was detected in Hope Valley (Fig. 4a). Similarly, primary productivity integrated over the water column was higher in 2013 throughout the entire study area (Fig. 4b), and the value was highest in Hope Valley, approximately five times higher than that in 2012. Despite being downstream from nutrient-rich water from the Bering Sea, the algal biomass and primary productivity in Hope Valley were comparable to or higher than those in the Bering Strait during both years. The increases in algal biomass and primary productivity from 2012 to 2013 would have been related to a change in water stratification, which is described in detail in Sect. 3.2.3.

3.2.2 Hotspot sections in 2012

A hydrographic section was obtained from the Bering Strait to the shelf slope of the Chukchi Sea along 168°45' W across the biological hotspot of the southern Chukchi Sea at ~68° N on 13–17 September 2012 (Fig. 5). We found a dome-like structure of bottom water characterised by an uplifted isohaline (isopycnal) surface at ~68° N with lower *T* and higher *S* (Fig. 5a), lower light transmission (Fig. 5b), and lower DO (Fig. 5c) than those of the surroundings.

We calculated f_{SIM} to examine the influence of BWW on the bottom water ($T = \sim -0.4$ °C, $S = \sim 33.2$) in the dome-like structure that was identified as BSAW. f_{SIM} had its minimum value north of 72° N at depths > 30 m above the Chukchi shelf slope (Fig. 5d). The negative f_{SIM} value means that the water was associated with brine rejection. The water there was characterised by near-freezing temperature and an *S* of ~33, and therefore, was identified as the BWW. The bottom water f_{SIM} at ~68° N was -0.05, smaller than that of the surrounding water ($f_{\text{SIM}} \sim 0$), suggesting that the BSAW in the dome-like structure was largely influenced by the BWW.

The nitrate concentration in this water (~7 μmol kg⁻¹) was lower than that of the Bering Strait (~20 μmol kg⁻¹; Fig. 5e). In contrast, the ammonium concentration was the highest in this bottom water (~12 μmol kg⁻¹; Fig. 5f). The ammonium concentration (~12 μmol kg⁻¹) reached 60% of the total inorganic nitrogen (TIN = nitrate + nitrite +

16369

ammonium) concentration (~20 μmol kg⁻¹) in this bottom water, and it was comparable to that in the Bering Strait. Other nutrients in this bottom water, i.e. phosphate and silicate, were also comparable to those in the Bering Strait.

We revisited the biological hotspot in the southern Chukchi Sea and conducted hydrographic and biogeochemical surveys on 3–4 October 2012 (Fig. 6). Similar to the previous survey in mid September, a dome-like structure of bottom water was found at ~68° N with lower *T* and higher *S* (Fig. 6a), lower light transmission (Fig. 6b), and lower DO (Fig. 6c) than those of the surrounding water. However, bottom water *T* was higher (-0.4 °C vs. ~0 °C), light transmission was lower (30% vs. 12%), and DO was lower (130 vs. 110 μmol kg⁻¹) than the values from the previous survey. Although the negative f_{SIM} value (~-0.03) suggests the influence of the BWW (Fig. 6d), its contribution decreased because both *T* and f_{SIM} increased slightly from mid September to early October. In general, light transmission and DO are higher in the BWW than in the BSAW because of the absence of particle inputs (less turbidity) and convection due to oxygen input during winter (Fig. 2b). Therefore, the decreases in light transmission and DO from mid September to early October were consistent with the decrease in the contribution of BWW to this bottom water. These changes in water properties were found in the mooring data when fluctuations of several days to a few weeks were detected, but the magnitudes of the fluctuations were smaller than the seasonal and significant yearly variation (Fig. 2). Therefore, the ship-based data represented the observed season and year.

The nitrate concentration in this water increased from 7 μmol kg⁻¹ in mid September to 16 μmol kg⁻¹ in early October (Fig. 6e). This may have been related to the changes in water composition described above and/or oxidation of ammonium (nitrification). The ammonium concentration remained high (~12 μmol kg⁻¹) in early October (Fig. 6f). The high ammonium level at this time suggests that ammonium production occurred at the bottom of the dome-like structure from mid-September to early October. This ammonium production contributed to an increase in the TIN concentration (28 μmol kg⁻¹) of the bottom water in early October 2012 in the biological hotspot of the southern

16370

in 2012 produced a prominent core of lower temperature and higher salinity (density) there compared to the surrounding area (Figs. 5a and 6a). However, the lack of a contribution by the BWW in 2013 resulted in a temperature and salinity similar to the surroundings (Fig. 7a).

5 Nutrient concentrations there were also controlled by the influences of the BSAW and BWW. In general, nutrient concentrations in the BSAW increase toward the south, in regions upstream of the flow (e.g. Springer and McRoy, 1993; Grebmeier et al., 2015), and nitrate concentration is $> 20 \mu\text{mol kg}^{-1}$ in the Gulf of Anadyr, where nutrient-rich Pacific waters are first advected up onto the Bering Sea shelf, which corresponds to
10 that in the nutrient maximum layer of the upper halocline of the Arctic (e.g. Jones and Anderson, 1986; Cooper et al., 1997). Similarly, the nitrate concentration in the BWW during winter was $\sim 20 \mu\text{mol kg}^{-1}$ because nutrients in the Bering and Chukchi shelves undergo little biological uptake during winter (Hansell et al., 1993; Cooper et al., 1997).
15 However, if the BWW remains on the Chukchi shelf until the next summer/fall, nutrients are supplied to the upper layer via vertical mixing and are used for biological production (Lowry et al., 2015; Nishino et al., 2015). As a result, this remnant BWW on the Chukchi shelf may have low nutrient concentrations, as observed at $72\text{--}73^\circ\text{N}$ near the shelf slope. The nitrate concentration there was $\leq 10 \mu\text{mol kg}^{-1}$ in the fall of both 2012 and
20 2013 (Figs. 5e and 7e). Therefore, the contribution to Hope Valley bottom water due to the remnant BWW, such as in 2012, could reduce nutrient concentrations there. In fact, the nitrate concentration there, which was a mixture of the BSAW and BWW in 2012 (Fig. 5e; $\sim 7 \mu\text{mol kg}^{-1}$), was lower than that of the bottom water identified as the BSAW without influence from the BWW in 2013 (Fig. 7e; $\sim 16 \mu\text{mol kg}^{-1}$).

25 Another important process controlling nutrient concentrations was ammonium production. Except for 2013, ammonium had maximum concentrations at the bottom of Hope Valley in the southern Chukchi Sea (Fig. 8f). In addition, the lowest light transmission and oxygen concentration were found there (Fig. 8b and c, respectively); i.e. a large amount of POM accumulated at the bottom of Hope Valley and its decomposition decreased oxygen and increased ammonium concentrations as a result of

16375

nutrient regeneration. The decomposing POM consumed oxygen and produced ammonium, generating a linear relationship between DO and ammonium concentrations in the southern Chukchi Sea (Fig. 9). The TIN at the bottom of Hope Valley in the fall of 2012 was comparable to that in the Bering Strait, which is located upstream of the
5 nutrient-rich BSAW flow. This high concentration ($\sim 20 \mu\text{mol kg}^{-1}$) was attributed to the high concentration of ammonium ($\sim 12 \mu\text{mol kg}^{-1}$), suggesting significant nutrient regeneration at the bottom, which explained 60% of the nutrient content. The TIN there in fall 2013 was $\sim 20 \mu\text{mol kg}^{-1}$ but ammonium was only $\sim 3 \mu\text{mol kg}^{-1}$, which does not support the scenario that nutrient regeneration at that time was lower than in fall 2012.
10 The weak stratification in fall 2013 may have diluted the ammonium levels via mixing with ammonium-free water in the upper layer, whereas bottom water nitrate was not diluted as much because nitrate in the upper layer was likely not depleted due to the influence of the BSAW. Therefore, it was difficult to estimate the contribution of nutrient regeneration to the nutrient content in the Hope Valley bottom water for 2013.
15 However, nutrient regeneration may have occurred significantly even in the fall 2013 because turbid water was still present, suggesting the accumulation of POM.

POM was largely carried by the BSAW during the fall of 2012 and 2013 and accumulated in the Hope Valley topographic depression. The nutrient regeneration caused by decay of POM at this site would help increase bottom water nutrient concentrations.
20 Furthermore, the dome-like structure lifts up the isopycnal surface, and nutrients would be supplied to the surface (euphotic zone) easier than to the surroundings. Vertical nutrient supply would be enhanced when stratification was weak, such as in 2013. For example, nitrogenous compounds are usually depleted at the sea surface where a relatively high level of ammonium ($\sim 1 \mu\text{mol kg}^{-1}$) was found in fall 2013, suggesting
25 nutrient regeneration at the bottom and vertical transport of the ammonium produced via vertical mixing (Fig. 7f). Indeed, the nutrient supply from the BSAW is important for the phytoplankton bloom during spring and early summer, as discussed by Springer and McRoy (1993). However, the combination of nutrient regeneration at the bottom and the uplifted isopycnal surface accompanied by the dome-like structure played an

16376

important role maintaining the high productivity of the biological hotspot in the southern Chukchi Sea at least during late summer and fall.

4.3 Stratification and primary productivity

Although Hope Valley maintained high primary productivity during late summer and fall, the magnitude was controlled by stratification of the water column. Primary productivity there was $0.3 \text{ g C m}^{-2} \text{ d}^{-1}$ in September 2012 and $1.6 \text{ g C m}^{-2} \text{ d}^{-1}$ in September 2013 (Figs. 3 and 4). The 2013 productivity was consistent with that estimated from in situ measurements during the same season from 2002 to 2004 ($1.4 \text{ g C m}^{-2} \text{ d}^{-1}$; Lee et al., 2007) and in 2007 ($1.6 \text{ g C m}^{-2} \text{ d}^{-1}$; Lee et al., 2013). The lower productivity in 2012 than in 2013 and in recent years was related to the strong stratification in 2012 caused by the high fraction of sea ice meltwater at the surface (Fig. 5d). Sea ice remained until September 2012 around Wrangel Island between the Chukchi and East Siberian Seas and may have resulted in the high fraction of sea ice meltwater at the surface of the Chukchi Sea, including the Hope Valley area.

Primary productivity in the Chukchi Sea in recent years seemed to decrease from that reported in the 1980s (Lee et al., 2007, 2013). Lee et al. (2007) hypothesised that the difference in primary productivity was associated with changes in water masses, the transport of nutrients with phytoplankton and sediments, primary productivity in the Bering Sea, and the large seasonal, annual, and geographical variation in primary productivity in the Chukchi Sea. Our results further suggest a large influence of sea ice meltwater in September 2012 on the reduction of primary productivity in the Chukchi Sea. Furthermore, data obtained in September 2009 indicated that high amounts of freshwater accumulated in the Chukchi Sea from Siberian coastal currents and negatively affected primary productivity (Yun et al., 2014). Such freshwater distributions, which control water column stratification, and thus primary productivity, are likely changed by wind- and buoyancy-forced currents on synoptic and seasonal time scales (Weingartner et al., 1999). Hence, synoptic and seasonal events could largely impact the fall bloom, and the frequency and magnitude of the bloom may not neces-

16377

sarily increase with a delay in fall freeze-up (longer ice-free season), as expected from satellite data (e.g. Arrigo et al., 2008; Pabi et al., 2008; Ardyna et al., 2014).

5 Summary

We analysed mooring and ship-based data obtained from a biological hotspot in the southern Chukchi Sea to understand water mass characteristics and their temporal changes, and how they influence phytoplankton biomass and productivity there. The mooring data indicated a seasonal change in water masses, i.e. the BSAW in summer/fall and BWW in winter/spring. The ship-based hydrographic and biogeochemical data suggested that the BSAW was largely modified by the BWW in fall 2012 but not during a typical fall (2004, 2008, 2010, and 2013). As a result, a prominent core of bottom water, which was characterised by lower temperature and higher salinity (density) than the surrounding water, was detected in 2012. The large influence of the BWW in 2012 would have reduced nutrient concentrations because nutrients in the BWW that had remained in the Chukchi Sea until summer/fall were probably used for the spring and fall blooms. In contrast, nutrient regeneration at the bottom increased nutrient concentrations and explained 60 % of the nutrient levels there in 2012. This high nutrient content, which was supplied by the BSAW and nutrient regeneration in the dome-like structure of the Hope Valley bottom water, maintained high primary productivity during the fall bloom. However, primary productivity was largely controlled by water column stratification characterised by the distribution of freshwater from sea ice meltwater and river water. Thus, there was large temporal and spatial variation in primary productivity and phytoplankton biomass. Therefore, long-term monitoring using moorings and chemical and biological sensors is necessary.

Although the mooring in this study was deployed only at the biological hotspot site in the southern Chukchi Sea, the data show a temporal change in phytoplankton biomass and related parameters for the first time. We observed spring and fall blooms associated with high Chl *a* concentrations. Before the fall bloom, turbidity increased and DO

16378

- Grebmeier, J. M., Bluhm, B. A., Cooper, L. W., Danielson, S. L., Arrigo, K. R., Blanchard, A. L., Clarke, J. T., Day, R. H., Frey, K. E., Gradinger, R. R., Kedra, M., Konar, B., Kuletz, K. J., Lee, S. H., Lovvorn, J. R., Norcross, B. L., and Okkonen, S. R.: Ecosystem characteristics and processes facilitating persistent macrobenthic biomass hotspots and associated benthivory in the Pacific Arctic, *Prog. Oceanogr.*, 136, 92–114, doi:10.1016/j.pocean.2015.05.006, 2015.
- Hama, T., Miyazaki, T., Ogawa, Y., Iwakuma, T., Takahashi, M., Otsuki, A., and Ichimura, S.: Measurement of photosynthetic production of a marine phytoplankton population using a stable ^{13}C isotope, *Mar. Biol.*, 73, 31–36, 1983.
- Hansell, D. A., Whitley, T. E., and Goering, J. J.: Patterns of nitrate utilization and new production over the Bering-Chukchi shelf, *Cont. Shelf Res.*, 13, 601–627, 1993.
- Hunt Jr., G. L., Blanchard, A. L., Boveng, P., Dalpadado, P., Drinkwater, K. F., Eisner, L., Hopcroft, R. R., Kovacs, K. M., Norcross, B. L., Renaud, P., Reigstad, M., Renner, M., Skjoldal, H. R., Whitehouse, A., and Woodgate, R. A.: The Barents and Chukchi Seas: Comparison of two Arctic shelf ecosystems, *J. Mar. Syst.*, 109–110, 43–68, doi:10.1016/j.jmarsys.2012.08.003, 2013.
- Hydes, D. J., Aoyama, M., Aminot, A., Bakker, K., Becker, S., Coverly, S., Daniel, A., Dickson, A. G., Grosso, O., Kerouel, R., van Ooijen, J., Sato, K., Tanhua, T., Woodward, E. M. S. and Zhang, J. Z.: Determination of dissolved nutrients (N, P, Si) in seawater with high precision and inter-comparability using gas-segmented continuous flow analysers, in: The GO-SHIP Repeat Hydrography Manual: A Collection of Expert Reports and Guidelines, IOCCP Report Number 14, ICPO Publication Series Number 134, edited by: Hood, E. M., Sabine, C. L., and Sloyan, B. M., UNESCO-IOC, Paris, France, available at: www.go-ship.org/HydroMan.html (last access: 25 September 2015), 2010.
- Jones, E. P. and Anderson, L. G.: On the origin of the chemical properties of the Arctic Ocean halocline, *J. Geophys. Res.*, 91, 10759–10767, 1986.
- Kawano, T.: Method for salinity (conductivity ratio) measurement, in: The GO-SHIP Repeat Hydrography Manual: A Collection of Expert Reports and Guidelines, IOCCP Report Number 14, ICPO Publication Series Number 134, edited by: Hood, E. M., Sabine, C. L., and Sloyan, B. M., UNESCO-IOC, Paris, France, available at: www.go-ship.org/HydroMan.html (last access: 25 September 2015), 2010.
- Kikuchi, T.: R/V *Mirai* Cruise Report MR12-E03, JAMSTEC, Yokosuka, Japan, available at: www.godac.jamstec.go.jp/cruisedata/mirai/e/index.html (last access: 25 September 2015), 2012.

16381

- Kinney, P., Arhelger, M. E., and Burrell, D. C.: Chemical characteristics of water masses in the American Basin of the Arctic Ocean, *J. Geophys. Res.*, 75, 4097–4104, 1970.
- Kwok, R., Cunningham, G. F., Wensnahan, M., Zwally, H. J., and Yi, D.: Thinning and volume loss of the Arctic Ocean sea ice cover: 2003–2008, *J. Geophys. Res.*, 114, C07005, doi:10.1029/2009JC005312, 2009.
- Lee, S. H., Whitley, T. E., and Kang, S. H.: Recent carbon and nitrogen uptake rates of phytoplankton in Bering Strait and the Chukchi Sea, *Cont. Shelf Res.*, 27, 2231–2249, doi:10.1016/j.csr.2007.05.009, 2007.
- Lee, S. H., Yun, M. S., Kim, B. K., Saitoh, S. I., Kang, C. K., Kang, S. H., and Whitley, T. E.: Latitudinal carbon productivity in the Bering and Chukchi seas during the summer in 2007, *Cont. Shelf Res.*, 59, 28–36, doi:10.1016/j.csr.2013.04.004, 2013.
- Lowry, K. E., Pickart, R. S., Mills, M. M., Brown, Z. W., vanDijken, G. L., Bates, N. R., and Arrigo, K. R.: The influence of winter water on phytoplankton blooms in the Chukchi Sea, *Deep-Sea Res. Pt. II*, 62, doi:10.1016/j.dsr2.2015.06.006, 2015.
- Mathis, J. T., Grebmeier, J. M., Hansell, D. A., Hopcroft, R. R., Kirchman, D. L., Lee, S. H., Moran, S. B., Bates, N. R., VanLaningham, S., Cross, J. N., and Cai, W.-J.: Carbon Biogeochemistry of the Western Arctic: Primary Production, Carbon Export and the Controls on Ocean Acidification, in: The Pacific Arctic region, Ecosystem Status and Trends in a Rapidly Changing Environment, edited by: Grebmeier, J. M. and Maslowski, W., Springer, Dordrecht, Netherlands, 223–268, doi:10.1007/978-94-017-8863-2, 2014.
- Matsuno, K., Yamaguchi, A., Nishino, S., Inoue, J., and Kikuchi, T.: Short-term changes in the mesozooplankton community and copepod gut pigment in the Chukchi Sea in autumn: reflections of a strong wind event, *Biogeosciences*, 12, 4005–4015, doi:10.5194/bg-12-4005-2015, 2015.
- McManus, D. A., Kelley, J. C., and Creager, J. S.: Continental Shelf Sedimentation in an Arctic Environment, *Geol. Soc. Am. Bull.*, 80, 1961–1984, 1969.
- McRoy, C. P.: ISHTAR, the project: an overview of Inner Shelf Transfer And Recycling in the Bering and Chukchi seas, *Cont. Shelf Res.*, 13, 473–479, 1993.
- Moran, S. B., Kelly, R. P., Hagstrom, K., Smith, J. N., Grebmeier, J. M., Cooper, L. W., Cota, G. F., Walsh, J. J., Bates, N. R., Hansell, D. A., Maslowski, W., Nelson, R. P., and Mulsow, S.: Seasonal changes in POC export flux in the Chukchi Sea and implications for water column-benthic coupling in Arctic shelves, *Deep-Sea Res. Pt. II*, 52, 3324–3343, 2005.

16382

Table 3. End-member values used in this study.

	Salinity	Potential Alkalinity ($\mu\text{mol kg}^{-1}$)
SIM (sea ice meltwater)	4	263
MW (meteoric water = river runoff + precipitation)	0	793
SE (saline end-member)	32.5	2223

16387

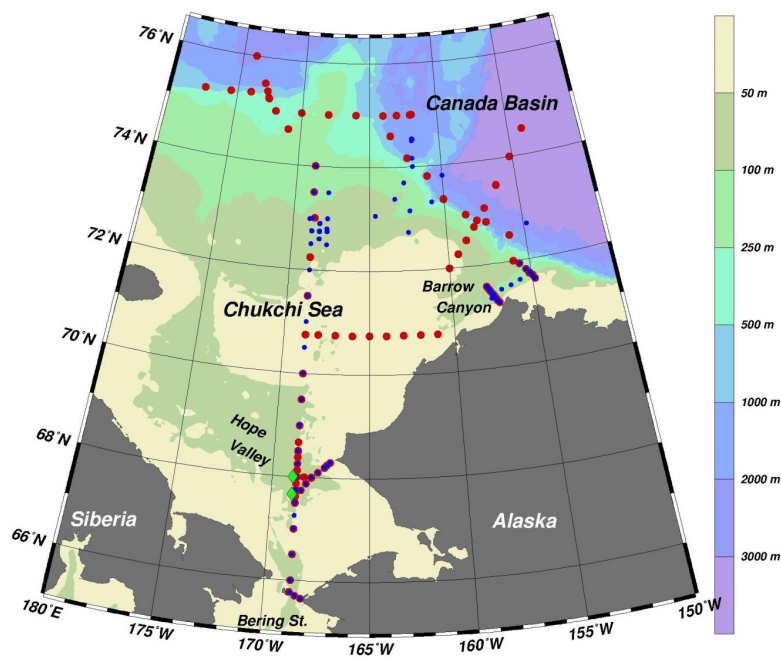


Figure 1. Map showing the bathymetric features of the study area and the hydrographic stations for the R/V *Mirai* cruises in 2012 (red dots) and 2013 (blue dots). Green diamonds represent the SCH-12 (southern site) and SCH-12-2/SCH-13 (northern site) mooring sites listed in Table 1.

16388

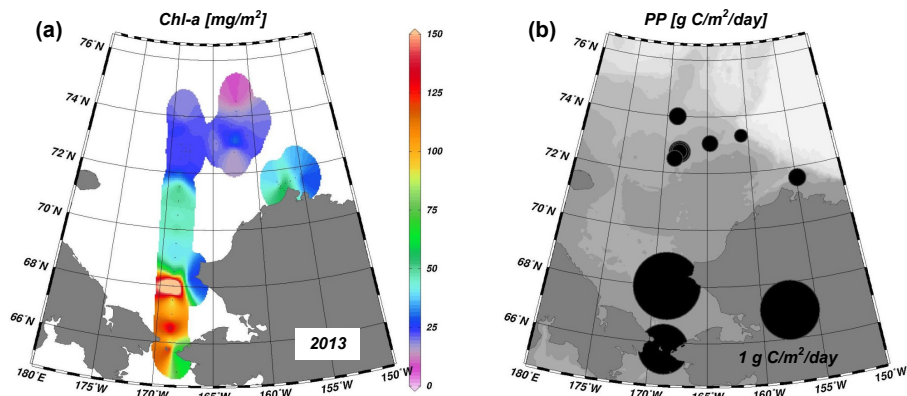


Figure 4. (a) Chlorophyll *a* integrated over the water column (mg m^{-2}) and (b) daily primary productivity in the water column ($\text{g C m}^{-2} \text{d}^{-1}$) obtained from the 2013 R/V *Mirai* cruise.

16391

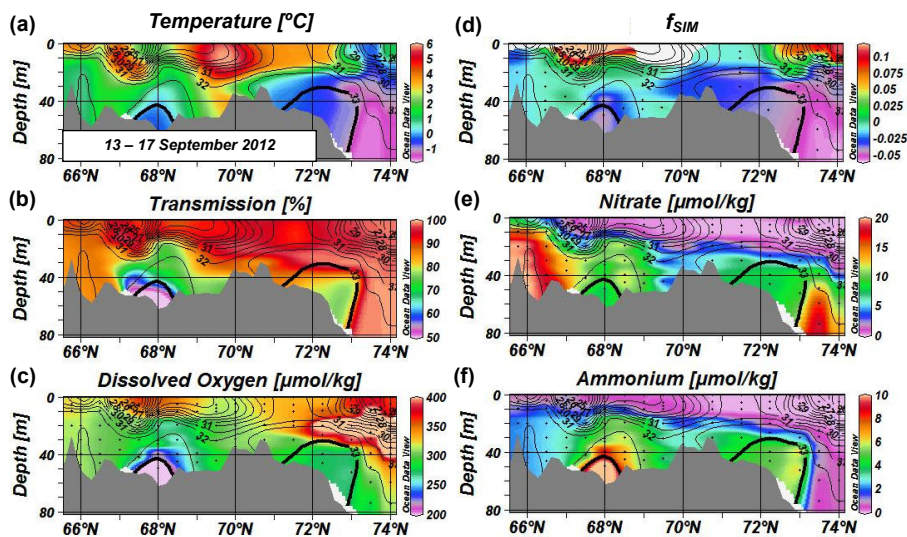


Figure 5. Vertical sections of (a) temperature ($^{\circ}\text{C}$), (b) light transmission (%), (c) dissolved oxygen ($\mu\text{mol kg}^{-1}$), (d) fraction of sea ice meltwater, (e) nitrate ($\mu\text{mol kg}^{-1}$), and (f) ammonium ($\mu\text{mol kg}^{-1}$) along the $168^{\circ}45' \text{W}$ meridian near the US–Russia border obtained during the 13–17 September 2012 R/V *Mirai* cruise. The water sampling level at each station is indicated by a black dot. Salinity contours are superimposed on each section with a 0.5 contour interval. The thick contour in each section indicates a salinity of 33.

16392

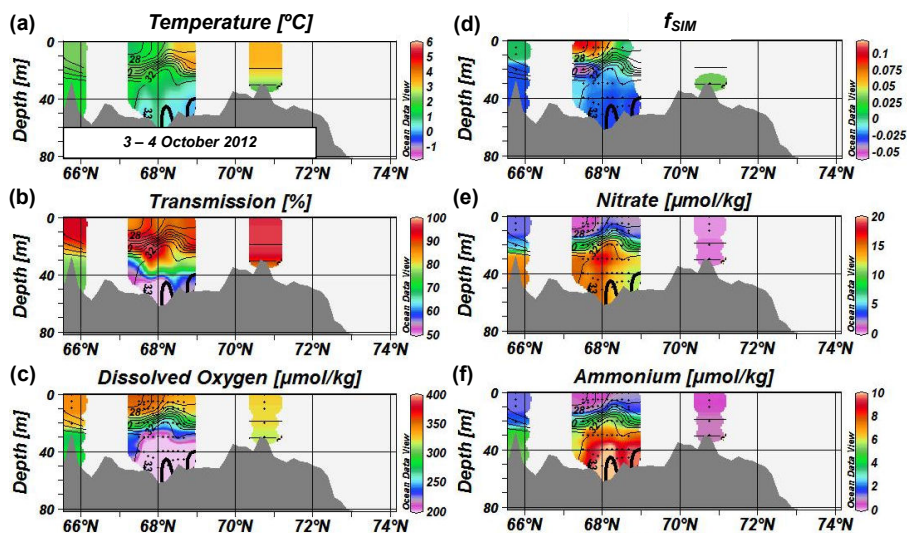


Figure 6. Vertical sections of (a) temperature ($^{\circ}\text{C}$), (b) light transmission (%), (c) dissolved oxygen ($\mu\text{mol kg}^{-1}$), (d) fraction of sea ice meltwater, (e) nitrate ($\mu\text{mol kg}^{-1}$), and (f) ammonium ($\mu\text{mol kg}^{-1}$) along the $168^{\circ}45'$ W meridian near the US–Russia border obtained during the 3–4 October 2012 R/V *Mirai* cruise. The water sampling level at each station is indicated by a black dot. Salinity contours are superimposed on each section with a 0.5 contour interval. The thick contour in each section indicates a salinity of 33.

16393

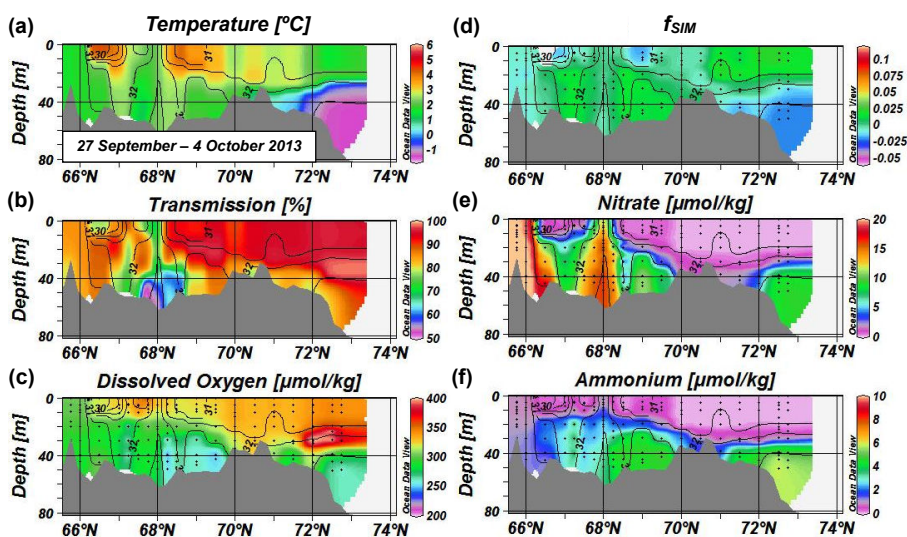


Figure 7. Vertical sections of (a) temperature ($^{\circ}\text{C}$), (b) light transmission (%), (c) dissolved oxygen ($\mu\text{mol kg}^{-1}$), (d) fraction of sea ice meltwater, (e) nitrate ($\mu\text{mol kg}^{-1}$), and (f) ammonium ($\mu\text{mol kg}^{-1}$) along the $168^{\circ}45'$ W meridian near the US–Russia border obtained during the 27 September–4 October 2013 R/V *Mirai* cruise. The water sampling level at each station is indicated by a black dot. Salinity contours are superimposed on each section with a 0.5 contour interval.

16394

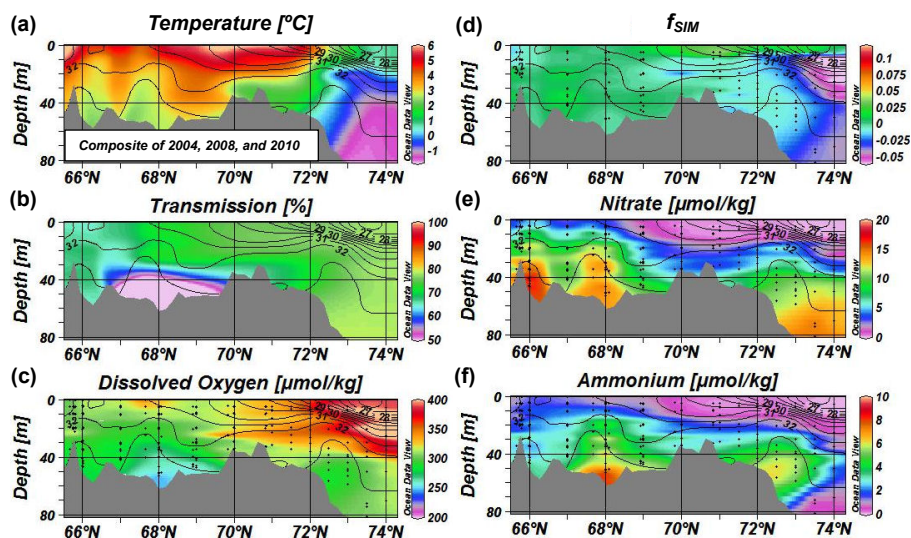


Figure 8. Vertical sections of (a) temperature ($^{\circ}\text{C}$), (b) light transmission (%), (c) dissolved oxygen ($\mu\text{mol kg}^{-1}$), (d) fraction of sea ice meltwater, (e) nitrate ($\mu\text{mol kg}^{-1}$), and (f) ammonium ($\mu\text{mol kg}^{-1}$) along the $168^{\circ}45' \text{ W}$ meridian near the US–Russia border obtained from composite data during the late summer to fall of 2004, 2008, and 2010 R/V *Mirai* cruises. In (b), the data were available only for 2004, and had a negative bias of $\sim 20\%$. The water sampling level at each station is indicated by a black dot. Salinity contours are superimposed on each section with a 0.5 contour interval.

16395

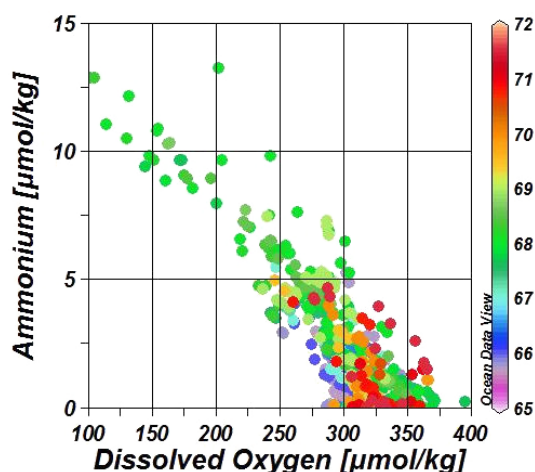


Figure 9. Diagram of dissolved oxygen ($\mu\text{mol kg}^{-1}$) and ammonium ($\mu\text{mol kg}^{-1}$) in the southern Chukchi Sea ($65\text{--}72^{\circ} \text{ N}$, $168^{\circ}45' \text{ W}$). Colour indicates latitude. Data were obtained from the late summer to fall 2004, 2008, 2010, 2012, and 2013 R/V *Mirai* cruises.

16396